



## Review

## Fine structure behaviour of VVER-1000 RPV materials under irradiation

B.A. Gurovich, E.A. Kuleshova, Ya.I. Shtrombakh, D.Yu. Erak, A.A. Chernobaeva\*, O.O. Zabusov

Russian Research Centre 'Kurchatov Institute', Kurchatov Sq. 1, Moscow 123182, Russia

## ARTICLE INFO

## Article history:

Received 5 August 2008

Accepted 2 February 2009

## ABSTRACT

Changes in the fine structure and mechanical properties of the base metal (BM) and weld metal (WM) of VVER-1000 pressure vessels during accumulation of neutron dose in the range of fluences  $\sim(3.2\text{--}15) \times 10^{23} \text{ m}^{-2}$  ( $E > 0.5 \text{ MeV}$ ) at 290 °C are studied using methods of transmission electron microscopy, fractographic analysis, and Auger electron spectroscopy. A correlation was found between the changes of mechanical properties and the micro- and nano-structures of the studied steels. Accumulation of neutron dose considerably raises the strength characteristics and transition temperature of VVER-1000 pressure vessel steels. The rate of changes in the mechanical properties of the weld metal is significantly higher than that of the base metal. The slower growth of strength characteristics and transition temperature shift of the base metal under irradiation as compared with the weld metal is due to the slower growth of the density of radiation defects and radiation-induced precipitates. The level of intergranular embrittlement under irradiation in the weld metal is not higher than in the base metal in spite of the higher content of nickel.

© 2009 Elsevier B.V. All rights reserved.

## Contents

1. Introduction .....	490
2. Materials .....	491
3. Experiments .....	491
4. Results .....	492
4.1. Mechanical tests .....	492
4.2. Micro-structure studies .....	492
4.3. Transmission electron microscopy studies (TEM) .....	492
4.4. Fractographic studies .....	492
4.5. Auger electron spectroscopy studies of grain-boundary segregations of phosphorus .....	492
5. Discussion .....	495
6. Conclusions .....	495
Acknowledgements .....	495
References .....	495

## 1. Introduction

Information on the micro- and nano-structure of reactor pressure vessel materials irradiated by fast neutrons is very important for development of physical models of radiation embrittlement of these materials. Systematic studies of the fine structure of irradiated pressure vessel materials have been carrying out in the Russian Research Center 'Kurchatov Institute' for many years. The main results of these studies are published in [1–7].

A number of studies carried out in Kurchatov Institute in the last five years were aimed at clarification of the fine structure

changes in reactor pressure vessel (RPV) materials under the action of operation factors (such as a flux of fast neutrons and temperature). The central idea of these studies is accumulation of transmission electron microscopy (TEM) and fractographic data on pressure vessel materials irradiated in a wide range of fast neutron fluences for each material. Such problem definition allows revealing of RPV fine structure behaviour during accumulation of neutron dose.

The subject of these studies was the metal of VVER-440 RPV surveillance specimens. Some of the results of these studies are published in [7,8].

In this paper, changes in the fine structure and mechanical properties of the VVER-1000 base metal (BM) and weld metal (WM) during accumulation of neutron dose in the range of fast neutron fluences  $\sim(3 \div 15) \times 10^{23} \text{ m}^{-2}$  ( $E > 0.5 \text{ MeV}$ ) are studied

\* Corresponding author. Tel.: +7 495 9472431; fax: +7 499 1961701.  
E-mail address: [anna.chernobaeva@gmail.com](mailto:anna.chernobaeva@gmail.com) (A.A. Chernobaeva).

using methods of TEM, fractographic analysis and Auger electron spectroscopy.

## 2. Materials

The subjects of our studies were VVER-1000 base and weld metals. Specimens of the base metal were taken from the shell of 15Kh2NMFA-A steel. The material of the weld joints was Sv-12Kh2N2MAA steel. Both of these materials were prepared according to the standard technology for VVER-1000 pressure vessels. The chemical composition of these steels is presented in Table 1.

Fig. 1 shows the range of concentrations of nickel, manganese, silicon, phosphorus, and copper in the irradiated shells and weld joints of Russian and Ukrainian VVER-1000 RPVs. Black dots show concentrations of these elements in the studied materials.

The chemical compositions of the studied materials is typical for the base metal and the weld metal of VVER-1000 RPVs. Concentration of Ni reaches the upper limit in the base metal and almost the upper limit in the weld metal. Thus, in terms of manufacturing technology and chemical composition, the selected materials may be considered representative for analyzing the structure and mechanical properties of the base metal and the weld metal of the most critical (high nickel) VVER-1000 RPVs.

## 3. Experiments

Charpy specimens of the base and weld metals were irradiated in a commercial reactor VVER-1000 at 290 °C. The parameters of irradiation are listed in Table 2. The specimens were located closer to the active zone than the reactor wall during irradiation. For this reason, the fast neutron fluxes on the specimens are 25–50× higher than the values typical for irradiation of VVER-1000 pressure vessel walls.

Embrittlement after irradiation was evaluated by the shift of critical embrittlement temperature ( $\Delta T_K$ ) in the tests of standard Charpy specimens [9].

Static uniaxial tensile tests were conducted to evaluate the strength characteristics of the studied materials. All tensile test specimens were prepared from halves of Charpy specimens.

The micro-structure of materials was studied using unirradiated polished specimens etched in solution of 3% nitric acid in methanol.

An electron microscope TEMSCAN-200CX (Jeol, Japan) with an acceleration voltage of 120 kV was used for transmission electron microscopy (TEM) studies. Specimens for transmission electron microscopy studies were cut from the halves of tested Charpy specimens on an electro-erosion rig and polished on a Struers rig (Austria) at  $-(70 \pm 60)$  °C using an electrolyte consisting of 10% of HClO<sub>4</sub> and 90% of methanol.

To determine the density of radiation-induced defects and precipitates, the thickness of specimens in the studied segment was measured using the method based on diffraction of electrons in a convergent beam [10], which provides accuracy better than 5%.

The halves of tested Charpy specimens were used for fractographic studies. The specimens were selected and vacuum-treated immediately after tests for preserving their surface of fracture. The radioactive version of the X-ray micro-analyzer SXR-50 (Cameca, France) installed in a hot cell was used to study the surfaces of frac-

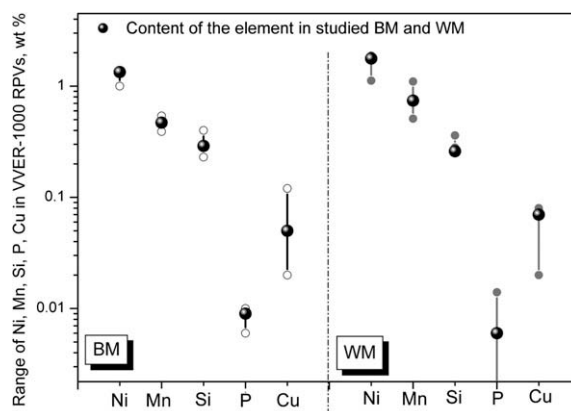


Fig. 1. Concentrations of Ni, Mn, Si, and Cu in the base metal and weld metal of VVER-1000 pressure vessels and concentrations of these elements in the studied materials.

Table 2  
Parameters of irradiation.

Material	$T_{\text{irr}}$ (°C)	$F(E > 0.5 \text{ MeV}) \times 10^{23} \text{ m}^{-2}$	Flux ( $E > 0.5 \text{ MeV}) \times 10^{16} \text{ m}^{-2} \text{ s}^{-1}$
BM	290±2	7.1	2–4
	290±2	9.5	2–4
	290±2	14.8	4–5
	290±2	3.1	2–4
WM	290±2	5.2	2–4
	290±2	5.6	2–4
	290±2	6.5	2–4
	290±2	11.6	4–5

ture. Images of fractures were obtained in secondary electrons under an acceleration voltage of 20 kV and a scanning probe current of 0.9 nA in the 50–1500 magnification range. Glagolev's method [11] was used to estimate the share of areas with different types of fractures (ductile transcrystalline fracture, brittle intercrystalline fracture, ductile intercrystalline fracture, cleavage, and quasicleavage) in the total surface of fracture after Charpy tests at different temperatures. The absolute error of measurements with a confidence probability of 95% did not exceed 5%.

Specimens of  $(1.3 \times 1 \times 15) \text{ mm}^3$  with a thin 0.3 mm-deep notch were prepared for Auger electron spectroscopy (AES) studies. Specimens were fractured immediately in the vacuum chamber of the Auger spectrometer MICROLAB Mk II in ultrahigh vacuum conditions with liquid-nitrogen cooling.

A special procedure was used in order to correctly determine the P content at the grain boundary (GB) [12]. Specimens of the unirradiated base metal of VVER-1000 pressure vessels were prepared for calibration measurements. The specimens were subjected to several special types of heat treatment for promoting P segregation to the grain boundary. Auger electron spectroscopy measurements of the P content at the grain boundary were performed for different types of heat treatment. The P content was also calculated using McLean's equilibrium segregation theory with taking into account co-segregation of Ni [13]. The obtained

Table 1  
Chemical composition of investigated pressure vessel materials, mass%.

Materials	C	Si	Mn	P	S	Cr	Ni	Mo	Cu	V
Fe-balance										
BM	0.17	0.29	0.47	0.009	0.014	2.24	1.34	0.51	0.05	0.09
WM	0.08	0.26	0.74	0.006	0.013	1.80	1.77	0.64	0.07	0.02

reference values were used for calculation of the phosphorus concentrations of at the grain boundaries of irradiated specimens.

## 4. Results

### 4.1. Mechanical tests

Figs. 2 and 3 show the changes in the values of yield point ( $\Delta R_{p0.2}$ ) and transition temperature shift ( $\Delta T_K$ ) of tensile test specimens and Charpy specimens correspondingly after irradiation by different fast neutron fluences.

The parameters of curves in these graphs were estimated using the least-square method.

Base metal	Weld metal
$\Delta R_{p0.2} = 16.9 \times (F \times 10^{22})^{0.4}$	
$\Delta T_K = 6.2 \times (F \times 10^{22})^{0.5}$	$\Delta T_K = 1.6 \times F \times 10^{22}$

where  $F$  is the fluence of fast neutrons ( $\text{m}^{-2}$ ).

Analysis of the results of mechanical tests shows the following:

- Accumulation of damaging irradiation dose leads to a considerable increase in the strength characteristics and critical embrittlement temperature of materials.
- The rate of changes in the properties of the weld metal is significantly higher than that of the base metal.
- Increase of the fluence of fast neutrons decreases the rate of growth of the strength characteristics and critical embrittlement temperature of the base metal. Increase of transition temperature shift of the weld metal is close to linear.

### 4.2. Micro-structure studies

Studies of the base and weld metals have shown that their micro-structure is bainite typical for Russian steels VVER-1000 [1–7]. The size of hereditary austenite grains varies in the range of 100–250  $\mu\text{m}$  and is also typical for VVER-1000 RPV steels [1–7].

### 4.3. Transmission electron microscopy studies (TEM)

Typical areas of the fine structure of the studied specimens are shown in Fig. 4. The results of TEM studies are presented in Table 3 and Figs. 2 and 3.

The obtained results make it possible to discover a number of regularities and specific features of radiation-induced structural changes in VVER-1000 RPV steels.

Radiation defects in the form of ‘black dots’ and dislocation loops with a resolved zero-contrast line are observed in steels after irradiation.

Disk-shaped precipitates are presented in the base metal. This type of precipitates is identified as chromium enriched carbides [14]. The density of chromium carbides remains practically the same with the growth of fluence up to  $\sim 1 \times 10^{24} \text{ m}^{-2}$ . After irradiation up to a higher fluence,<sup>1</sup> the density of disk-shaped precipitates grows to a certain extent and their sizes decrease. This may be an indication that a new population of smaller radiation-induced carbides is formed with fluence increase (см. таблиц. 3) with somewhat higher density and smaller average sizes. Radiation-induced carbides were not found in weld joints in the studied range of fluences.

Round nano-sized precipitates were detected in irradiated specimens of the base metal and the weld metal. Such precipitates are completely absent in unirradiated materials. These precipitates are

homogeneously distributed in metal grains, and their average size reaches 3–5 nm. The special samples for Atom probe tomography (APT) investigation were cut out from the same halves of tested Charpy specimens. APT study was performed at Oak Ridge National Laboratory (ORNL) [15]. The results of this study show that the precipitates found in the weld metal are enriched with Ni, Mn and Si atoms (Ni–Mn–Si precipitates) and the precipitates found in the base metal are enriched with Ni and Si atoms (Ni–Si precipitates). In earlier work the same materials, irradiated to fluence  $2.4 \times 10^{23} \text{ m}^{-2}$  ( $E > 0.5 \text{ MeV}$ ) in Ford reactor were studied in ORNL by APT. The results of this study have been reported in [16,17]. The similar type of precipitates was described in [18–23].

The average size of rounded precipitates does not change when the irradiation dose is increased up to  $5.2 \times 10^{23} \text{ m}^{-2}$  for the weld metal and up to  $9.5 \times 10^{23} \text{ m}^{-2}$  for the base metal and starts to grow upon further increase of the irradiation dose.

The volume density of rounded precipitates grows almost linearly in the entire range of fluences. The rate of growth of precipitates density and its absolute values in the weld metal are much higher than in the base metal.

The diameters of radiation-induced dislocation loops in the base metal remain the same in the entire studied range of fluences. The density of dislocation loops in the base metal slightly increases with the growth of fluence from  $7.1 \times 10^{23} \text{ m}^{-2}$  to  $9.5 \times 10^{23} \text{ m}^{-2}$  and increases 2–3 $\times$  upon further growth of fluence up to  $\sim 14.8 \times 10^{23} \text{ m}^{-2}$ .

The diameters of radiation-induced dislocation loops in the weld metal do not change when fluence grows from  $3.1 \times 10^{23} \text{ m}^{-2}$  to  $5.2 \times 10^{23} \text{ m}^{-2}$  and somewhat increases upon further growth of fluence up to  $\sim 11.6 \times 10^{23} \text{ m}^{-2}$ .

The density of dislocation loops in the weld metal slightly increases with the growth of fluence from  $3.1 \times 10^{23} \text{ m}^{-2}$  to  $5.2 \times 10^{23} \text{ m}^{-2}$  and increases 2 $\times$  with the growth of fluence up to  $\sim 6.5 \times 10^{23} \text{ m}^{-2}$ . Further growth of the irradiation doses up to  $\sim 11.6 \times 10^{23} \text{ m}^{-2}$  increases the density of dislocation loops in 30–40 times.

### 4.4. Fractographic studies

The results of fractographic studies are presented in Table 4 and Fig. 5. The results presented in Table 4 show that:

- The share of ductile transcrystalline fracture in all studied fractures correlates with normalized values of absorbed energy ( $A/A_{\text{max}}$ , where  $A$  – absorbed energy value for a given test temperature,  $A_{\text{max}}$  – maximum absorbed energy).
- Intergranular areas appear in fractures of irradiated specimens. This structural component of fractures is absent in unirradiated specimens.
- The share of intercrystalline fracture in the base metal and weld metal are practically the same at comparable fluences and increases with the irradiation dose.

### 4.5. Auger electron spectroscopy studies of grain-boundary segregations of phosphorus

The fracture surfaces of the base metal and the weld metal were studied by means of Auger electron spectroscopy (AES). The average concentration of phosphorus was equal to  $19.6 \pm 2.7\%$  of monolayer coverage at boundaries of the base metal grains irradiated with doses of up to  $14.9 \times 10^{23} \text{ m}^{-2}$  and  $15.2 \pm 1.5\%$  of monolayer coverage at the boundaries of the weld metal grains irradiated with doses of up to  $11.5 \times 10^{23} \text{ m}^{-2}$ .

Experimental data on phosphorus content in the grain boundaries were not obtained because fracture surfaces of small unirradiated specimens did not contain intergranular fracture areas. But

<sup>1</sup> The specified value of fluence is approximately two times higher than the designed lifetime fluence for the shell and welds of the VVER-1000 opposite core.

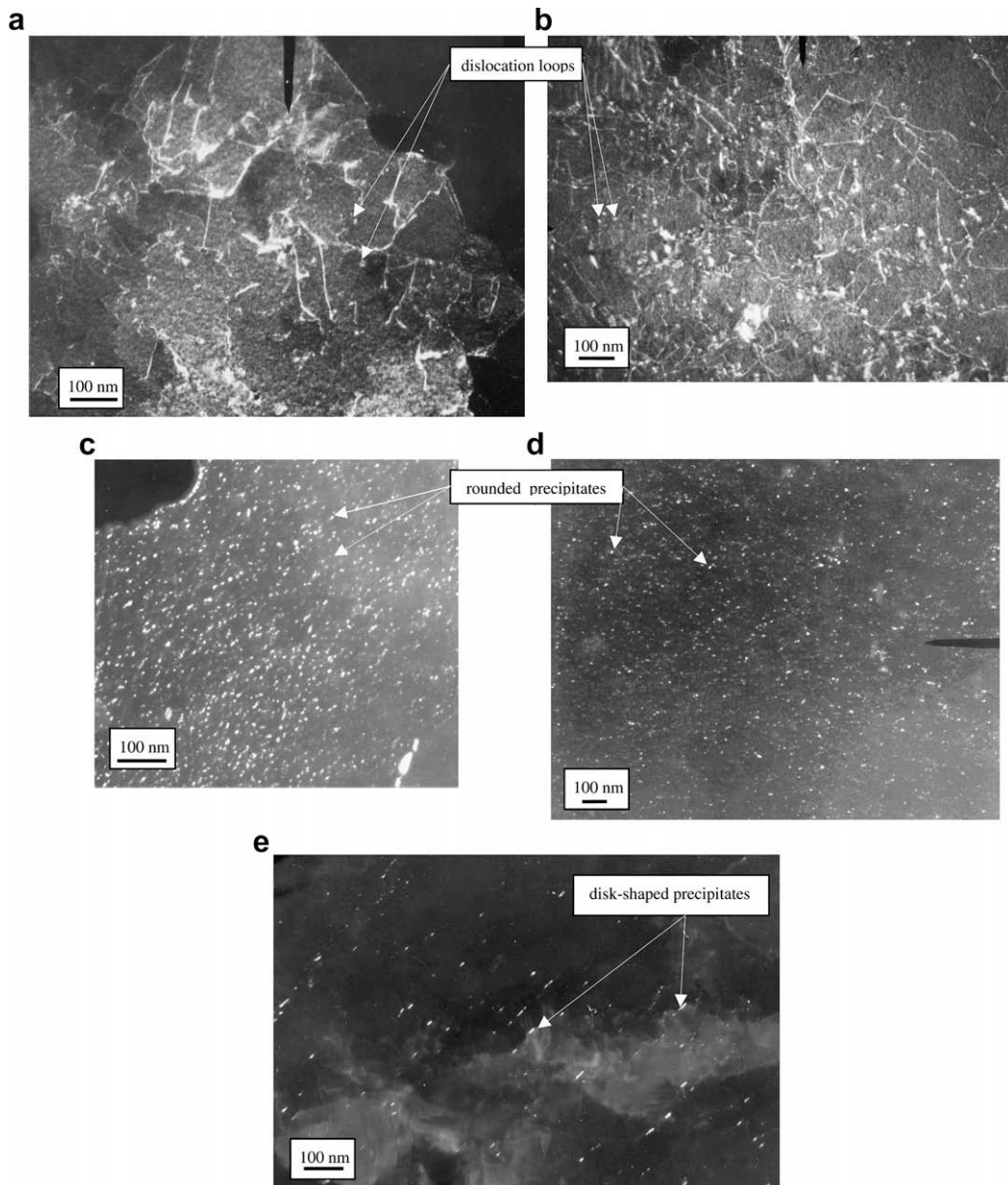


**Fig. 2.** TEM micrographs (dark-field images) of the fine structure of VVER-1000 base metal ( $F = 1.47 \times 10^{24} \text{ m}^{-2}$ ) and weld metal ( $F = 1.16 \times 10^{24} \text{ m}^{-2}$ ): radiation defects – dislocation loops (a) base metal (b) weld metal; rounded precipitates (c) base metal (d) –weld metal (e) disk-shaped precipitates in base metal.

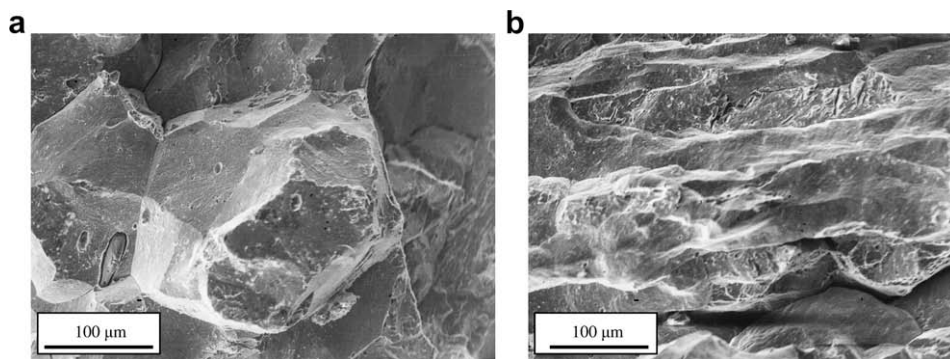


**Fig. 3.** SEM micrograph of brittle intergranular fracture surface: (a) base metal (irradiated up to  $F = 1.47 \times 10^{24} \text{ m}^{-2}$ ); (b) weld metal (irradiated up to  $F = 1.16 \times 10^{24} \text{ m}^{-2}$ ).

calculations by McLean model of equilibrium segregations [McLean] predict 3–4% of monolayer coverage for both the base and weld metals after the initial heat treatment. Thus the irradiation

caused an increase in the phosphorus grain-boundary segregation level in the both materials with the corresponding increase in intergranular fracture area share (see Table 4).



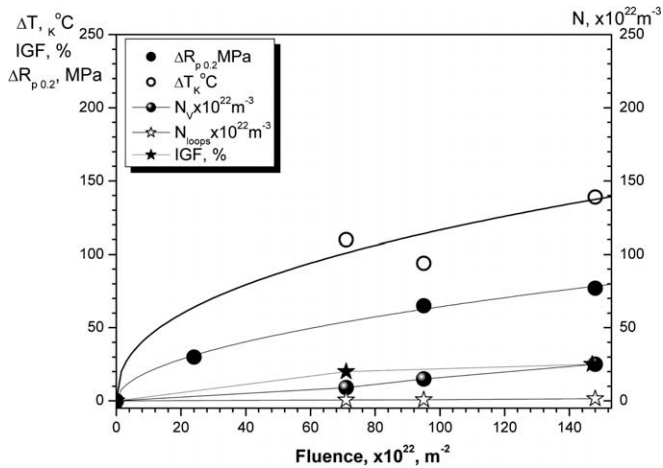


Fig. 4. Changes of transition temperature, yield stress, density of precipitates and dislocation loops and part of inter-crystalline fracture in base metal under irradiation.

According to an estimate made in [24] a change of phosphorus concentration at the grain boundary must lead to the following shift of  $T_K$ :

$$\Delta T_K = [42 + 78 \ln(d/d_0)] \Delta C_p^{\Gamma^3} \quad (1)$$

where  $d$  is the grain size,  $\mu\text{m}$ , and  $d_0$  is a characteristic quantity equal to  $1 \mu\text{m}$ . For both the base metal and weld metal, the grain size may be assumed to be equal to  $200 \mu\text{m}$  as the measured values were in the range  $150\text{--}250 \mu\text{m}$ . Therefore, when the concentration of phosphorus at the grain boundary increases by 1 at.%, the shift of

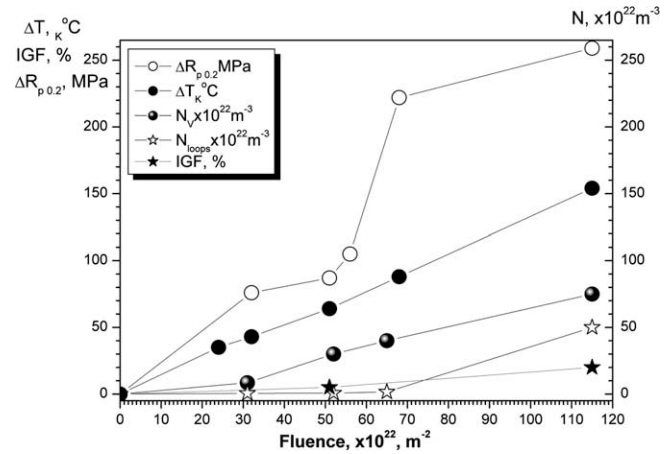


Fig. 5. Changes of transition temperature, yield stress, density of precipitates and dislocation loops and part of inter-crystalline fracture in weld metal under irradiation.

$T_K$  must be approximately  $4\text{--}5 \text{ }^\circ\text{C}$ . Thus, the estimation shows that the increase in phosphorus content in the grain boundaries could lead to a certain raise in  $T_K$ .

The studied materials were subjected to accelerated irradiation, whereas the fast neutron flux in real pressure vessels are 1 or 2 orders of magnitude lower. The level of intercrystalline segregation at the fast neutron flux densities corresponding to real operation conditions may almost exceed the level of intercrystalline segregation during accelerated irradiation due to longer irradiation time and, according to the estimate above, could cause a considerable DBTT shift.

Table 3  
Data on densities and average sizes of radiation defects, radiation-induced disk-shaped and rounded precipitates.

N°	Fluence ( $\times 10^{23} \text{ m}^{-2}$ )	Density of dislocation loops ( $10^{21} \text{ m}^{-3}$ )	Diameter of dislocation loops nm	Density of disk-shaped precipitates ( $10^{21} \text{ m}^{-3}$ )	Diameter of disk-shaped precipitates (nm)	Density of rounded precipitates ( $10^{21} \text{ m}^{-3}$ )	Diameter of rounded precipitates (nm)
<i>Base metal (Ni = 1.34%, Mn = 0.47%, Si = 0.29%)</i>							
1	7.1	5–6	4–5	3–5	15–20	80–100	2–3
2	9.5	7–8	4–5	3–5	15–20	100–200	2–3
3	14.8	10–20	4–5	4–6	10–15	200–300	3–4
<i>Weld metal (Ni = 1.77%, Mn = 0.74%, Si = 0.26%)</i>							
4	3.1	5–6	4–5	–	–	70–90	2–3
5	5.2	6–7	4–5	–	–	200–400	2–3
6	6.5	10–20	5–6	–	–	300–500	3–4
7	11.6	400–600	6–8	–	–	700–800	3–5

Table 4  
Summary data of fractographic analysis results for investigated Charpy specimens.

Fluence ( $\times 10^{23} \text{ m}^{-2}$ ), $T_K$ ( $^\circ\text{C}$ )	$T_{\text{test}}$ ( $^\circ\text{C}$ )	Absorbed energy (J)	Fraction of different fracture modes (%)				
			Ductile	Quasicleavage	Cleavage	Brittle intergranular fracture	Ductile intergranular fracture
<i>Base metal (P = 0.009%, Cu = 0.05%, Ni = 1.34, Mn = 0.47%, Si = 0.29%)</i>							
$F = 0$	–90	57	20	70	10	–	–
$T_K = -82$	–100	13	Traces	90	10	–	–
$F = 7.1$	–12.5	64	45	30	10	15	–
$T_K = -25$	0	64	45	25	10	20	–
$F = 14.8$	–18	45	25	40	10	25	–
$T_K = -10$	–12.5	53	35	30	10	25	–
<i>Weld metal (P = 0.006%, Cu = 0.07%, Ni = 1.77%, Mn = 0.74%, Si = 0.26%)</i>							
$F = 0$	–75	25	15	80	5	–	–
$T_K = -59$	–55	55	40	55	5	–	–
$F = 5.2$	–12.5	42	30	60	5	5	–
$T_K = 2$	0	50	35	60	5	Traces	–
$F = 11.6$	50	19	20	50	5	20	–
$T_K = 94$	87.5	41	40	20	5	20	–

## 5. Discussion

The results obtained in this work (Figs. 2 and 3) reveal the following features of VVER-1000 pressure vessel steel behaviour under irradiation:

- Formation of dislocation loops and gradual increase of their density in the base metal in the entire studied range of fluences.
- Formation of dislocation loops, gradual increase of their density in the weld metal up to a fluence of  $\sim 6.5 \times 10^{23} \text{ m}^{-2}$ , and sharp increase of their density (by a factor of 30–40) in the weld metal in the range of fast neutron fluences  $\sim (6.5\text{--}11.6) \times 10^{23} \text{ m}^{-2}$ .
- Formation of round precipitates (Ni–Mn–Si precipitates in the weld metal and Ni–Si precipitates in the base metal). The density of precipitates grows almost linearly in the entire studied range of fluences. The rate of growth of the density of precipitates and its absolute values in the weld metal are much higher than in the base metal.
- No changes in the density of disk-shaped precipitates (chromium-enriched carbides) in the base metal (up to a fluence of  $9.5 \times 10^{23} \text{ m}^{-2}$ ) and formation of a new conglomerate of carbides upon further growth of fluence up to  $\sim 14.8 \times 10^{23} \text{ m}^{-2}$ .
- Absence of radiation-induced carbides in the weld metal.
- Formation of grain-boundary segregations of impurities, first of all phosphorus, resulting in the formation of areas of brittle intercrystalline fractures.

The rates of growth of the critical embrittlement temperature are different for the base and weld metals due to the complex changes in the structure of these metals.

Fine structure parameters for different states and the corresponding shifts of critical embrittlement temperature ( $\Delta T_K$ ) are presented in Figs. 2 and 3 to evaluate the contribution of different radiation-induced changes in the structure of the base metal and the weld metal to radiation-induced embrittlement.

The concentrations of phosphorus at the grain boundaries in the base metal and weld metal are close within the measurement error. The grain size in the weld metal is approximately twice as large as in the base metal. The change in the yield point under irradiation and its absolute value for the weld metal ( $R_{p0.2} = 795 \text{ MPa}$ ,  $\Delta R_{p0.2} = 259 \text{ MPa}$ ) are higher than for the base metal ( $R_{p0.2} = 751 \text{ MPa}$ ,  $\Delta R_{p0.2} = 139 \text{ MPa}$ ). In this situation, the share of intergranular fracture in the weld metal must be larger than in the base metal.

Estimation of contributions of different mechanisms to radiation-induced embrittlement requires comparison between the rate of growth of each of them and their influence on the variation of  $\Delta T_K$  in the base metal and weld metal.

The growth of the densities of rounded precipitates in the base metal and weld metal is not the only factor which affects the rise of critical embrittlement temperature of VVER-1000 RPV steels under irradiation. The changes of properties under irradiation are apparently caused by the complex combined action of different structural elements. At the first stages of irradiation, embrittlement of both the base metal and weld metal is mainly caused by formation of radiation-induced nickel-enriched precipitates, grain-boundary segregation of phosphorus. The density of dislocation loops at the early stage of irradiation does not increase significantly for the base metal and weld metal; simultaneously the rate of growth of the density of the rounded precipitates does not change as well. At higher fluencies the density of dislocation loops increases: by a factor of  $\sim 30\text{--}40$  in the weld metal at  $11.6 \times 10^{23} \text{ m}^{-2}$  and by a factor of 1.5 in the base metal at  $14.8 \times 10^{23} \text{ m}^{-2}$  with continuous increase in the round precipitates density. It results in a considerable difference in the rates of embrittlement of weld and base metals. The function  $\Delta T_K$  linearly depends on fluence for the weld metal and rate of  $\Delta T_K$  increase slows down for the base metal.

Thus at high fluences of fast neutrons, intensification of radiation-induced embrittlement is mainly related to radiation hardening, namely, the increase of the concentration of radiation defects with further growth of the concentration of the rounded precipitates in the weld metal, and mainly the growth of the concentration of the rounded precipitates in the base metal.

Comparison of the obtained results with the results previously published in [7,8] for VVER-440 RPV steels shows that the main salient feature in the nano-structure of RPV steels under irradiation is the fact that the density of radiation-induced round precipitates does not decrease in VVER-1000 RPV steels, whereas in VVER-440 RPV steels the density of round precipitates drops after irradiation to fluence of  $\sim 1.3 \times 10^{24} \text{ m}^{-2}$ . The difference may be explained by the high content of alloying elements, whose atoms participate in the formation of precipitates in VVER-1000 RPV steels. As long as the contents of manganese and silicon are practically the same in the respective materials of VVER-440 and VVER-1000, the main difference is the content of nickel, which is much higher in VVER-1000 materials.

## 6. Conclusions

1. The micro- and nano-structures of VVER-1000 pressure vessel steels were studied in relation to the changes in the mechanical properties of the base metal and weld metal of VVER-1000 pressure vessels after irradiation with fluences of up to  $(11.6\text{--}14.8) \times 10^{23} \text{ m}^{-2}$  at  $\sim 290 \text{ }^\circ\text{C}$ .
2. A correlation was found between the changes of mechanical properties and the micro- and nano-structures of the studied steels.
3. Accumulation of neutron dose considerably raises the strength characteristics and transition temperature of VVER-1000 pressure vessel steels. The rate of changes in the mechanical properties of the weld metal is significantly higher than that of the base metal.
4. The slower growth of strength characteristics and transition temperature shift of the base metal under irradiation, as compared to the weld metal, is due to the slower growth of the density of radiation defects and radiation-induced precipitates.
5. The increase of the density of radiation defects and the growth of the density of radiation-induced precipitates result in the linear dependence of transition temperature shift on fluence of the weld metal under irradiation without slowdown of its embrittlement rate.
6. The weld metal does not demonstrate higher intergranular embrittlement under irradiation than the base metal in spite of the higher content of nickel.

## Acknowledgements

This study was funded by ISTC and performed within the ISTC Project No. 3420 and State Contract No. 02.523.12.3012 in frame of FASI projects.

## References

- [1] B.A. Gurovich, E.A. Kuleshova, O.V. Lavrenchuk, J. Nucl. Mater. 228 (1996) 330.
- [2] B.A. Gurovich, E.A. Kuleshova, Yu.A. Nikolaev, Ya.I. Shtrombakh, J. Nucl. Mater. 246 (1997) 91.
- [3] B.A. Gurovich, E.A. Kuleshova, K.E. Prihodko, Ya.I. Shtrombakh, J. Nucl. Mater. 264 (1998) 333.
- [4] B.A. Gurovich, Yu.N. Korolev, E.A. Kuleshova, Yu.A. Nikolaev, Ya. I. Shtrombakh, in: R.K. Nanstad, M.L. Hamilton, F.A. Garner, A.S. Kumar (Eds.), Effects of Radiation on Materials, ASTM STP 1325, American Society for Testing and Materials, Philadelphia, 1999, pp. 271.
- [5] B.A. Gurovich, E.A. Kuleshova, Ya.I. Shtrombakh, O.O. Zabusov, E.A. Krasikov, J. Nucl. Mater. 279 (2–3) (2000) 59.

- [6] E.A. Kuleshova, B.A. Gurovich, Ya.I. Shtrombakh, D.Yu. Erak, O.V. Lavrenchuk, J. Nucl. Mater. 300 (2002) 127.
- [7] E.A. Kuleshova, B.A. Gurovich, Ya.I. Shtrombakh, Yu.A. Nikolaev, V.A. Pechenkin, J. Nucl. Mater. 342 (1–3) (2005) 77.
- [8] B.A. Gurovich, E.A. Kuleshova, Ya.I. Shtrombakh, Yu.A. Nikolaev, Evolution of the nanostructure of VVER-440 and VVER-1000 pressure vessels steels irradiated in a broad range of fast neutron fluences, in: Proceedings of the 10th International Conference on Material Issues in Design, Manufacturing and Operation of Nuclear Power Plants Equipment, 2008, pp. 48–57 (in Russian).
- [9] Regulations for Strength Calculations of Equipment and Pipelines of Atomic Power Plants (PNAE G-7-002-86), Energoatomizdat, Moscow, 1989.
- [10] P.M. Kelly, A. Jostsons, R.G. Blake, J.G. Napier, Phys. Status Solidi A 31 (1975) 771.
- [11] S.A. Saltykov, Stereometric Metallography, Metallurgiya, Moscow, 1976, 271 p.
- [12] O.O. Zabusov, A.A. Chernobaeva, Ya.I. Shtrombakh, Yu.A. Nikolaev, E.A. Kuleshova, M.K. Miller, K.F. Russell, R.K. Nanstad, VANT, Mater. Sci. New Mater. 2–71 (2008) 32 (in Russian).
- [13] M.P. Seah, Acta Metall. 25 (1977) 345.
- [14] M.K. Miller, R. Jayaram, K.F. Russell, J. Nucl. Mater. 225 (1995) 215.
- [15] M.K. Miller, K.F. Russell, R.K. Nanstad, A.A. Chernobaeva, O. Zabusov, Y. Shtrombakh, D. Erak, Atom probe tomography of VVER-1000 forging and weld metal irradiated to high fluence, degradation 2007, in: Proceedings of 13th International Conference on Environmental Degradation in Nuclear Power Systems, Whistler, British Columbia, August 2007.
- [16] R. Nanstad, M. Sokolov, M. Miller, Comparison of nickel effects on embrittlement mechanisms in a radiation-sensitive weld and in prototypic WWER-1000 and A533B steels, in: Proceeding of IAEA Meeting on Irradiation Effects and Mitigation in Reactor Pressure Vessel and RPV Internal, Kristal Goos, 2004.
- [17] IAEA-TECDOC-1441, Effects on Nickel on Irradiation Embrittlement of Light Water Reactor Pressure Vessel Steels, IAEA, Vienna, Austria, 2005.
- [18] M.K. Miller, K.F. Russell, J. Kocik, E. Keilova, J. Nucl. Mater. 282 (2000) 83.
- [19] M.K. Miller, K.F. Russell, J. Kocik, E. Keilova, Micron 32 (2001) 749.
- [20] П. Оже, С. Вэлвел, Д. Блаветт и Ф. Парейдж, «Радиационно-стимулированная сегрегация примесей в ферритных корпусных реакторных сталях: томографические атомно-зондовые исследования», Материалы первой московской международной школы физиков ИТЭФ, 1998, Москва (стр. 143–153).
- [21] Report NUREG/CR-6778, The effect of composition and heat treatment on hardening and embrittlement of reactor pressure vessel steels, US Nuclear regulatory commission office of Nuclear regulatory research, Washington, DC, 20555-0001.
- [22] M.G. Burke, R.J. Stofanak, J.M. Hyde, C.A. English, W.L. Server, Characterization of irradiation damage in A508 Gr4N forging steels, in: Proceedings of 10th International Conference on Environmental Degradation of Materials in Nuclear Power Systems – Water Reactors, Lake Tahoe, NV, 5–9 August 2001, NACE, 2002 (Electronic only).
- [23] E.D. Eason, G.R. Odette, R.K. Nanstad, T. Yamamoto, A physically based correlation of irradiation-induced transition temperature shifts for RPV steels, Prepared at Oak Ridge National Laboratory, Oak Ridge, Tennessee, managed by UT-Battelle, LLC, under Contract No. DE-AC05-00OR22725.
- [24] Yu.A. Nikolaev, Yu.R. Kevorkyan, O.O. Zabusov, Influence of radiation-stimulated grain-boundary segregation of phosphorus on the operational properties of nuclear-reactor-vessel materials, Atom. Energy 91 (5) (2001) 884.